scientific reports

Check for updates

OPEN

Disulfiram inhibits Gasdermin D pores formation and improves insulin-dependent glucose uptake and glucose homeostasis in skeletal muscle of obesity-induced insulin-resistant mice

Cynthia Cadagan[1,5], Javier Russell-Guzmán[2,5], Luan Américo-Da-Silva[1], Paula Montaña[1], Genaro Barrientos[3,4], Sonja Buvinic[1,3], Gladys Tapia[4], Manuel Estrada[4,6]✉ & Paola Llanos[1,3]✉

Insulin resistance (IR), which involves impaired insulin signaling diminished insulin sensitivity in skeletal muscle, is closely associated with chronic low-grade inflammation. A key mediator of this process is the NLRP3 inflammasome, which activates Gasdermin D (GSDMD). Upon cleavage, the N-terminal fragment of GSDMD (GSDMD-NT) forms membrane pores that facilitate interleukin-1β (IL-1β) release. Disulfiram (DSF), an FDA-approved drug that also inhibits GSDMD-NT pore formation, has emerged as a potential therapeutic for inflammasome-mediated inflammation. However, the role of GSDMD in skeletal muscle during IR remains poorly understood. This study evaluated whether GSDMD-NT-mediated IL-1β release contributes to skeletal muscle inflammation and IR, and whether DSF can restore insulin sensitivity. Male C57BL/6 mice were fed a normal chow diet (NCD) or a high-fat diet (HFD) for 8 weeks; a subgroup of HFD-fed mice received intraperitoneal DSF (50 mg/kg) for 3 weeks. The flexor digitorum brevis (FDB) and gastrocnemius muscles were collected for single-fiber isolation, quantitative PCR, immunoblotting, and immunofluorescence. IL-1β levels were measured by ELISA. Insulin sensitivity was assessed via 2-NBDG uptake, Akt phosphorylation, and glucose tolerance tests (IPGTT). HFD-fed mice exhibited increased GSDMD-NT and oligomer levels, localized to the sarcolemma and T-tubules, along with elevated IL-1β in skeletal muscle. DSF administration reduced weight gain, fasting glycemia, IPGTT, and systemic IL-1β, while enhancing insulin-stimulated 2-NBDG uptake and Akt phosphorylation in FDB. Moreover, DSF reduced GSDMD-NT oligomerization and IL-1β release in the gastrocnemius muscle. These findings suggest a novel pathogenic role for GSDMD in skeletal muscle IR and support DSF as a potential candidate for metabolic disease intervention.

Keywords GSDMD-NT, Glucose uptake, IL-1β release, Insulin signaling, NALP3 inflammasome

Abbreviations

AUC	Area under the curve
DSF	Disulfiram

[1]Institute for Research in Dental Sciences, Faculty of Dentistry, Universidad de Chile, Olivos 943, Independencia, Santiago 8380544, Chile. [2]Escuela de Kinesiología, Facultad de Salud, Universidad Santo Tomás, Av. Ejército 146, Santiago 8320000, Chile. [3]Centre for Exercise, Metabolism and Cancer Studies, Faculty of Medicine, CEMC, Universidad de Chile, Independencia 1027, Independencia, Santiago 8380000, Chile. [4]Institute of Biomedical Sciences, ICBM, Faculty of Medicine, Universidad de Chile, Independencia 1027, Independencia, Santiago 8380000, Chile. [5]Cynthia Cadagan and Javier Russell-Guzmán have contributed equally to the work. [6]This work is in memory of Dr. Manuel Estrada, our colleague, professor, co-investigator, and friend, who passed away during the course of this study. His contributions were fundamental to the conception and development of this research. His scientific insight, generosity, and unwavering commitment will continue to inspire us. ✉email: maestrada@uchile.cl; pllanos@odontologia.uchile.cl

DMSO	Dimethyl sulfoxide
FDB	Flexor digitorum brevis
GSDMD	Gasdermin D
GSDMD-NT	N-terminal fragment of Gasdermin D
GLUT4	Glucose transporter type 4
HFD	High-fat diet
IL-1β	Interleukin-1β
IPGTT	Intraperitoneal glucose tolerance test
IR	Insulin resistance
NCD	Normal-chow diet
NLRP3	NOD-, LRR-, pyrin domain-containing protein 3
S	Sarcolemma
T	Triads
TXNIP	Thioredoxin-interacting protein

Obesity is a multifactorial condition arising from the interplay of genetic, environmental, and lifestyle factors, and is associated with chronic metabolic dysfunction[1], a key driver of insulin resistance (IR)[2]. This metabolic impairment is closely linked to the development of type 2 diabetes mellitus, dyslipidemia, and cardiovascular disease, all of which are major contributors to global morbidity and mortality[3]. Skeletal muscle plays a central role in glucose homeostasis and serves as the primary site for insulin-stimulated glucose uptake[4]. Additionally, it functions as a source of proinflammatory cytokines, thereby linking obesity to systemic low-grade inflammation[5]. Chronic inflammation disrupts glucose homeostasis primarily by inducing insulin resistance, impairing insulin secretion, and increasing hepatic glucose output. These effects are mediated by inflammatory cytokines and immune cell activity in metabolic tissues, creating a self-reinforcing cycle that drives the development and progression of metabolic diseases such as type 2 diabetes[6]. A critical mechanism connecting innate immunity to metabolic dysfunction is the activation of inflammasomes, a multiprotein complex that drives the release of proinflammatory cytokines. Among these, the NLRP3 (NOD-, LRR-, pyrin domain-containing protein 3) inflammasome is the most extensively studied in chronic disease contexts, playing a central role through activation of caspase-1, which promotes the maturation and secretion of interleukin-1β (IL-1β)[7,8]. We recently demonstrated that NLRP3 components are expressed in skeletal muscle, where they contribute to impaired glucose metabolism and promote IR[9]. Skeletal muscle from IR-obese mice exhibited NLRP3 hyperactivation, increased IL-1β expression, and reduced GLUT4 translocation in insulin response, which were reversed by pharmacological inhibition of NLRP3[9].

Gasdermin D (GSDMD), a principal substrate of caspase-1, is a key effector of pyroptosis, a lytic proinflammatory form of programmed cell death downstream of NLRP3 activation[10]. Upon cleavage by caspase-1, the C-terminal inhibitory domain is removed, liberating the N-terminal fragment (GSDMD-NT), which oligomerizes and integrates into the plasma membrane to form pores. These pores facilitate the release of proinflammatory cytokines, notably IL-1β, also independently of complete cell lysis[11–13]. This sublytic activity provides a mechanism for sustained inflammatory signaling in metabolically active tissues. Previously, we observed increased full-length GSDMD protein abundance and localization in skeletal muscle fibers from high-fat diet (HFD)-fed mice[9], implicating a possible role for GSDMD in the pathogenesis of obesity-induced IR. By enabling cytokine release without overt pyroptosis, GSDMD may sustain a local proinflammatory milieu that impairs insulin signaling. Thus, the NLRP3–GSDMD axis emerges as a critical molecular link between obesity-induced inflammation and metabolic dysfunction in skeletal muscle.

Disulfiram (DSF), a pharmacological inhibitor of GSDMD-NT pore formation, has gained attention for suppressing inflammation downstream of NLRP3 activation, without interfering with upstream signaling pathways[14]. Originally approved by the FDA for the treatment of chronic alcoholism as an aldehyde dehydrogenase inhibitor[15]. DSF has recently demonstrated metabolic benefits in rodent models, including reductions in body weight, adiposity, hyperglycemia, and IR as well as reversal of HFD–induced hepatic steatosis[16]. Despite these promising systemic effects, the role of this compound in skeletal muscle insulin sensitivity has not been explored. An omics-based study showed that DSF modulates lipid metabolism, redox balance, and influences autophagic pathways in hepatic cells[17]. At the molecular level, DSF inhibits GSDMD-NT-dependent pore formation through covalent modification of a critical cysteine residue (Cys191 in humans, Cys192 in mice), which prevents oligomerization and IL-1β release without altering inflammasome assembly[17]. This selective inhibition of downstream pro-inflammatory signaling, while preserving innate immune sensing, positions DSF as a promising candidate for drug repurposing in metabolic disease. Nevertheless, its direct effects on skeletal muscle metabolism and insulin responsiveness remain to be elucidated.

In this study, we tested the hypothesis that GSDMD-NT contributes to IL-1β-mediated skeletal muscle inflammation and IR, and that pharmacological inhibition with DSF can restore insulin responsiveness by preventing GSDMD-NT oligomerization and pore formation. To address this, we employed HFD-fed mice, a well-established model of obesity-induced IR. This study aims to elucidate a novel mechanistic link between inflammasome activation and muscle insulin sensitivity, and to explore further the therapeutic potential of targeting GSDMD as a strategy to mitigate metabolic inflammation and improve glucose homeostasis.

Methods

Ethics statement

All animal procedures were approved by the Animal Bioethics Committee of the Faculty of Dentistry, University of Chile (Protocol CBA 240423 FOUCH). All methods were carried out in accordance with the recommendations of the Guide for the Care and Use of Laboratory Animals of the U.S. Department of Health and Human Services

and American Veterinary Medical Association (AVMA) guidelines. The selected procedures were designed to minimize discomfort and distress while allowing for the collection of relevant metabolic and molecular data. Additionally, the study is reported in accordance with the ARRIVE guidelines (https://arriveguidelines.org).

Animals

A total of 96 male C57BL/6 mice, provided by the Animal Facility of the Faculty of Dentistry at the University of Chile, were used in this study. Animals were specific-pathogen-free (SPF), with no prior procedures before enrollment in the study. Prior to procedures, animals were maintained at 21 °C with a 12:12-h light-dark cycle. Environmental enrichment was provided and included nesting materials, cardboard cones for shelter and exploration, and social housing with compatible animals. After 21 days, the animals were assigned to two groups: normal chow diet (NCD, $n = 35$), which received a standard diet (10% fat, 20% protein, and 70% carbohydrates). In contrast, the experimental group ($n = 35$) received, by 8 weeks, a high-fat diet (HFD) (60% fat, 20% protein, and 20% carbohydrates; D12492, Research Diets, New Brunswick, NJ, USA). A subgroup of HFD-fed mice ($n = 20$) received intraperitoneal injections of either vehicle (sunflower oil; HFD control) or disulfiram (HFD + DSF; Sigma-Aldrich, Burlington, MA, USA) at 50 mg/kg body weight, 3 times per week from week 7 to 10. A separate group of HFD-fed mice was allocated for ex vivo muscle incubation experiments ($n = 6$). Each experimental group was assigned a numerical code, and tissue collection was performed in a randomized order based on this coding. Handling procedures were consistent across groups to minimize potential bias. For euthanasia, animals were placed in a plexiglass chamber, anesthetized with 5% isoflurane for 5 min, and then subjected to cervical dislocation.

Intraperitoneal glucose tolerance test (IPGTT)

Following a 4-hour fast, mice received an intraperitoneal glucose bolus (2 g/kg). Blood glucose levels were measured from tail vein samples at 0, 15, 30, 60, and 120 min using a One Touch II glucometer (Lifescan, Johnson & Johnson, Switzerland).

Culture of isolated skeletal muscle fibers

As previously described by[18], isolated fibers from the flexor digitorum brevis (FDB) muscle were obtained through enzymatic digestion with IV collagenase (Worthington, USA) for 90 min at 37 °C. Next, muscle tissue was mechanically dissociated by passing it through fire-polished Pasteur pipettes. The resulting fibers were plated on coverslips coated with Matrigel (Sigma-Aldrich, Burlington, MA, USA) and cultured in DMEM (25 mM glucose), supplemented with 10% horse serum (Invitrogen, Waltham, MA, USA). Cultures were maintained in an incubator at 37 °C, 95% humidity, and 5% CO_2.

2-NBDG uptake

The assay was performed as reported previously[18]. Isolated FDB muscle fibers were cultured for 24 h in serum-free DMEM, incubated for 5 min in glucose-free Krebs – Ringer buffer, and then stimulated with insulin (100 nM, Actrapid, Novo Nordisk, Denmark) for 20 min. Fibers were exposed to fluorescent glucose analog 2-[N-(7-nitrobenz-2-oxa-1,3-diazol-4-yl) amino]−2-deoxy-D-glucose (2-NBDG, 300 µM; Invitrogen, Waltham, MA, USA) for 15 min, washed, and transferred to Krebs – Ringer buffer with 5.6 mM glucose. Intracellular fluorescence images were acquired using a Cell Observer Z1 epifluorescence microscope (Carl Zeiss AG, Germany). The probe was excited at 488 nm, and the resulting emission was recorded at 525 nm using a bandpass filter, with a 40X objective (numerical aperture 0.55) and a 0.63X adapter. Fluorescence intensity was calculated by averaging intracellular signal measurements from 3 distinct regions of each fiber and subtracting the background fluorescence signal recorded in the extracellular medium. Approximately 128 individual fibers were analyzed for each condition. Image analysis and region of interest (ROI) quantification were performed using Fiji software (NIH, Bethesda, MD, USA).

GLUT4-7*myc*-eGFP electroporation in FDB muscle

Plasmid injection and electroporation were performed as described[19,20]. Briefly, FDB muscles from HFD-fed mice were injected with 2 mg/mL hyaluronidase and 1 h later the muscles were injected again with a total of 20 µg of GLUT4-7*myc*-eGFP plasmid. This construct contains a *myc*-epitope in an exofacial domain and an eGFP-tag, allowing for quantification of cell surface GLUT4[21]. A pair of electrodes was placed under the skin and oriented parallel to each other and perpendicular to the long axis of the foot. ~100 V/cm, 20 pulses, 20 ms in duration each, at 1 Hz frequency were generated using a SQ wave electroporator ECM 630 (BTX; Harvard Apparatus, Holliston, MA, USA). The expression of GLUT4-7*myc*-eGFP was assayed 10 days after electroporation.

GLUT4-7*myc*-eGFP translocation assays

Fiber electroporated with GLUT4-7*myc*-eGFP chimera plasmids were seeded on glass coverslips followed by serum deprivation for 3 h. Cells were preincubated for overnight with 10 nM DSF, 100 nM insulin for 20 min (Actrapid, Novo-Nordisk, Denmark) or both. Labeling of surface GLUT4-7*myc*-eGFP in nonpermeabilized cells was performed as described[9,20]. Briefly, after washing with PBS, fibers were fixed by incubation for 10 min at room temperature with PBS containing 4% paraformaldehyde (Electron Microscopy Science, Hatfield, PA, USA). Next, skeletal muscle fibers were rinsed with PBS and blocked for 1 h with PBS-1% BSA at room temperature. GLUT4-7*myc*-eGFP levels in the cell surface were detected with the monoclonal anti-*myc* antibody (1/100 dilution, SC-40; Santa Cruz Bio-technology, Santa Cruz, CA, USA) followed by treatment with a secondary antibody conjugated with AlexaFluor 635 (1/500 dilution, Molecular Probes, Invitrogen, Carlsbad, CA, USA). Images were obtained using a C2 + confocal microscope system (Nikon Instruments Inc., Minato, Tokyo, Japan). GLUT4-7*myc*-eGFP translocation analysis was performed as described[22].

MTT viability assay

Cell viability was assessed using the MTT reduction assay. Adult skeletal muscle fiber cultures were incubated in supplemented DMEM containing 0.5 mg/mL MTT for 20–30 min at 37 °C to allow mitochondrial dehydrogenases in viable cells to reduce MTT to insoluble formazan crystals. The reaction was stopped by adding an equal volume of 10% SDS prepared in 10 mM HCl, followed by overnight incubation at room temperature to ensure complete solubilization of formazan. Absorbance was measured at 570 nm using an Infinite F50 microplate reader (Tecan, Switzerland).

mRNA expression

Total RNA was extracted from FDB muscles using TRIzol® reagent (Invitrogen, USA), following the manufacturer's protocol. Complementary DNA (cDNA) was synthesized via reverse transcription using 1 µg of total RNA and random primers. Quantitative PCR (qPCR) was carried out as previously described[9], employing the following primers (Integrated DNA Technologies, Ann Arbor, MI, USA): GSDMD (forward: TGAAGCAC GTCTTGGAACAG; reverse: TCTTTTCATCCCAGCAGTCC). Expression levels were normalized against the housekeeping gene Rplp0 (forward: CTCCAAGCAGATGCAGCAGA; reverse: ATAGCCTTGCGCATCATGG T) and quantified using the $2^{-\Delta\Delta Ct}$ method.

Western blotting

Tissue samples were lysed using a manual homogenizer and sonication at 4 °C in RIPA buffer. Next, lysates were centrifuged at 3,000 × g for 15 min. Protein (30–60 µg) from FDB and gastrocnemius samples, respectively, was resolved on 10% to 15% SDS–PAGE gels. The proteins were transferred to PVDF membranes and blocked with 5% bovine serum albumin (BSA). The membranes were incubated overnight at 4 °C with the following primary antibodies: NLRP3 (1:500, anti-rat, R&D System, Minneapolis, MN, USA), Caspase-1 (1:500, anti-mouse), ASC (1:500, anti-mouse) from Santa Cruz Biotechnology, Inc (Dallas, TX, USA), IL-1β (1:500, anti-rabbit), β-tubulin (1:2,000, anti-rabbit), GAPDH (1:10,000, anti-rabbit), phospho-Akt Ser473 (1:2,000, anti-rabbit), and total Akt (1:2,000, anti-rabbit), all from Cell Signaling Technology (Danvers, MA, USA); and GSDMD-NT (1:500, anti-rabbit, Abcam, Cambridge, MA). After incubation with species-specific secondary antibodies for 2 h, protein bands were visualized using the LI–COR Odyssey® XF imaging system and Image Studio software (Lincoln, NE, USA). Densitometric analyses were performed using Fiji software (NIH, Bethesda, MD, USA), and figures were prepared using the Sciugo platform.

Evaluation of GSDMD oligomers

To assess GSDMD oligomerization in FDB or gastrocnemius muscle, homogenate samples were initially incubated for 5 min with 10 µg/mL catalase (Sigma-Aldrich, Burlington, MA, USA), followed by 10 min incubation in cold phosphate-buffered saline (PBS) containing 100 mM N–ethylmaleimide (NEM; Sigma-Aldrich, Burlington, MA, USA) at 4 °C to alkylate free cysteine residues. Tissue homogenization was then carried out at 4 °C using a handheld homogenizer (D1000, Biolab, Madrid, Spain), followed by sonication in cold RIPA lysis buffer (Sigma-Aldrich, Burlington, MA, USA) supplemented with protease inhibitors (Basilea, Switzerland) and 100 mM NEM. Lysis and supernatant collection were carried out as previously described for Western blot analysis. To evaluate the effect of DSF, gastrocnemius muscles from HFD-fed mice were enzymatically dissociated with type IV collagenase for 30 min and cultured ex vivo for 24 h in the presence or absence of 10 nM DSF.

Microsomal fractionation

Skeletal muscles from the trunk and lower limbs of NCD– or HFD–fed mice were homogenized using an Ultra–Turrax® homogenizer (IKA, Germany) in buffer A (150 mM KCl, 5 mM $MgSO_4$, 20 mM MOPS/Tris, pH 6.8) containing protease inhibitors [leupeptin (1 µg/mL), pepstatin (1 µg/mL), benzamidine (0.4 mM), and phenylmethylsulfonyl fluoride (1 mM)]. Homogenates were centrifuged at 1,380 × g for 30 min at 4 °C. Pellets were re-extracted, and the combined supernatant was centrifuged at 17,000 × g for 30 min at 4 °C to isolate membrane fractions. Pellets were resuspended in buffer A and centrifuged again at 1,380 x g to remove contractile proteins. The resulting supernatant was subjected to a second 17,000 x g centrifugation for 30 min at 4 °C. The final pellet, enriched in triad structures (T–tubule), was washed in buffer B (300 mM sucrose, 20 mM MOPS/Tris, pH 6.8) with protease inhibitors, centrifuged again, resuspended in a minimal volume of buffer B, snap-frozen in liquid nitrogen, and stored at – 80 °C[23].

Immunofluorescence imaging

Isolated FDB fibers plated on 12 mm Matrigel–coated coverslips were fixed in 4% paraformaldehyde, permeabilized with 0.01% Triton X-100, and blocked in 1% BSA/PBS for 1 h. Fibers were incubated overnight at 4 °C with primary antibodies against anti-GSDMD-NT (1:300, anti-rabbit, Abcam, Cambridge, MA), anti-NLRP3 (1:500, R&D Systems, Minneapolis, MN, USA), and anti-DPHR (1:500, Invitrogen, Waltham, MA, USA), followed by Alexa Fluor-conjugated secondary antibodies (1:250, Invitrogen, Waltham, MA, USA) for 1 h. Fluorescence images were acquired using a Nikon C2 + confocal microscope (40X, NA 1.3) and analyzed using Fiji software (NIH, Bethesda, MD, USA).

Caspase-1 activity

Caspase-1 activity was measured in isolated FDB muscle fibers using the FLICA 660-YVAD-FMK Caspase-1 Assay Kit (Immunochemistry Technologies, Davis, CA, USA) following the manufacturer's instructions. After the stimulation protocol, fibers were incubated with the FLICA probe (1:30 dilution in culture medium) for 30 min at 37 °C in the dark, washed twice with 1X FLICA wash buffer, fixed with 4% paraformaldehyde in PBS, and mounted on glass slides. Confocal images (3–12 per condition) were acquired 16–24 h after probe

addition using a C2 + confocal microscope (Nikon Instruments Inc., Tokyo, Japan). Fluorescence intensity was quantified using Fiji (NIH, USA) by subtracting background fluorescence measured outside the fiber from the mean intensity of three regions of interest within the fiber.

IL-1β levels in plasma and cultured muscle fibers

Plasma levels of IL-1β in NCD, HFD, and HFD + DSF mice were determined using a commercial ELISA kit (R&D Systems, USA) according to the manufacturer's instructions. To assess IL-1β in culture media of muscle fibers, FDB and gastrocnemius muscle from NCD and HFD mice were digested with type IV collagenase for 30 min and cultured for 24 h with or without 10 nM DSF. IL-1β levels were normalized to muscle weight (pg/mg).

Statistical analysis

Data are presented as mean ± SEM. Comparisons between and within multiple groups were assessed using two-way ANOVA followed by Tukey *post-hoc* test. The Mann–Whitney *U* test was used to compare two independent groups, and the Wilcoxon signed-rank test was applied for paired comparisons of cultures derived from the same animal under two distinct conditions. A $p < 0.05$ was considered statistically significant. All analyses and graphical representations were performed using GraphPad Prism 9 (GraphPad Software Inc., San Diego, CA, USA).

Results

Elevated GSDMD-NT protein levels in skeletal muscle from HFD-fed mice

The GSDMD-NT protein assembles into oligomeric pores that facilitate IL-1β release and has been recognized as a novel downstream target of NLRP3 inflammasome activation across various cell types, including macrophages[24] and skeletal muscle[9]. To corroborate whether chronic exposure to a high-fat diet (HFD) activates this pathway in skeletal muscle, we first evaluated the protein content of NLRP3 inflammasome components and caspase-1 activation, which are upstream regulators of GSDMD-NT. The levels of NLRP3, ASC, and cleaved caspase-1 were all increased in skeletal muscle from HFD-fed mice compared with controls. Consistently, caspase-1 activity was also significantly elevated in the HFD group (Fig. Supp. 1). Next, we analyzed whether GSDMD-NT was differentially expressed in the skeletal muscle of obesity-induced IR mice. As shown in Fig. 1, no significant differences were observed in the mRNA expression levels of GSDMD in muscle fibers isolated from HFD-fed mice compared to NCD-fed mice (Fig. 1a). Nevertheless, we detected an immunoreactive band at 30 kDa for the GSDMD-NT protein, which was significantly increased ($p = 0.032$) in HFD-fed mice (2.76 ± 0.43-fold) compared to NCD-fed mice (1.00 ± 0.34-fold), as determined by Western blot analysis in FDB muscle homogenates (Fig. 1b). In addition, we analyzed the localization of GSDMD-NT in isolated skeletal muscle fibers (Fig. 1c). Immunofluorescence detection of the GSDMD-NT and NLRP3 proteins showed an increased fluorescence intensity for both proteins in isolated fibers from HFD-fed mice compared to NCD-fed mice. Of note, immunostaining experiments revealed a peripheral signal in the medial portion of the skeletal fibers (Fig. Supp. 2). To determine whether GSDMD-NT co-localizes with DHPR, a well-established marker of the T-tubule membrane, we performed immunostaining and Western blot analysis on both the isolated microsomal fraction (enriched in sarcolemma membranes) and the triad membrane (enriched in T-tubules flanked by sarcoplasmic reticulum). As shown in Figure Supp. 3, GSDMD-NT co-localizes with DHPR in HFD-fed mice, reaching an M1 Manders coefficient of 0.98 ± 0.01, compared to NCD-fed mice (0.90 ± 0.05, Fig. Suppl. 3b). In addition, we detected an immunoreactive band in the Western Blotting analysis of GSDMD-NT in both the microsomal fraction and T-tubule membrane, with increased signal in membranes isolated from HFD-fed mice compared to NCD-fed mice (Fig. Suppl. 3c).

An HFD induces oligomerization of GSDMD-NT and enhances IL-1β release in skeletal muscle

It has been suggested that GSDMD-NT monomers can be inserted into the plasma membrane and subsequently assembled into pore-forming oligomers, facilitating the release of inflammatory mediators such as IL-1β. We performed Western blot analysis using a non-denaturing gel to assess whether this process also occurs in skeletal muscle. A significant increase ($p = 0.029$) in the oligomer-to-monomer ratio was observed in HFD-fed mice compared to NCD-fed mice (4.08 ± 0.89-fold and 1.00 ± 0.22-fold, respectively) (Fig. 2a), indicating increased pore assembly in skeletal muscle. Subsequently, we measured IL-1β release in ex vivo FDB and gastrocnemius muscle (Fig. 2b & Fig. Suppl. 4). IL-1β levels were significantly elevated in HFD-fed mice, reaching values of 2.29 ± 0.44 pg/mg protein in the FDB ($p = 0.018$) and 0.66 ± 0.05 pg/mg protein in the gastrocnemius ($p = 0.032$), compared to 1.10 ± 0.16 pg/mg and 0.48 ± 0.05 pg/mg, respectively, in NCD-fed controls. Despite the increase levels of GSDMD-NT oligomers observed in muscle from HFD-fed mice compared to controls, no differences in fiber viability were detected by the MTT assay (Fig. Suppl. 5). These results suggest that GSDMD-NT oligomerization could lead to IL-1β release in skeletal muscle from obesity-induced IR mice, without lysis of the muscle fibers.

Disulfiram treatment improves glucose tolerance and reduces plasma IL-1β levels in HFD-fed mice

To investigate the effects of DSF on glucose handling and plasma IL-1β levels, we intraperitoneally injected HFD-fed mice three times per week with DSF (50 mg/kg) or vehicle for 3 weeks. Before treatment, the HFD-fed group exhibited similar body mass, fasting blood glucose, and IPGTT (Fig. Suppl. 6). Post-treatment, mice injected with either DSF or vehicle showed no significant changes in food intake or insulinemia (Fig. 3). In contrast, DSF treatment reduced both total body mass ($p = 0.027$) and epididymal adipose tissue ($p = 0.026$), restored fasting blood glucose levels ($p < 0.0001$), which remained significantly elevated in vehicle-treated mice, and led to an

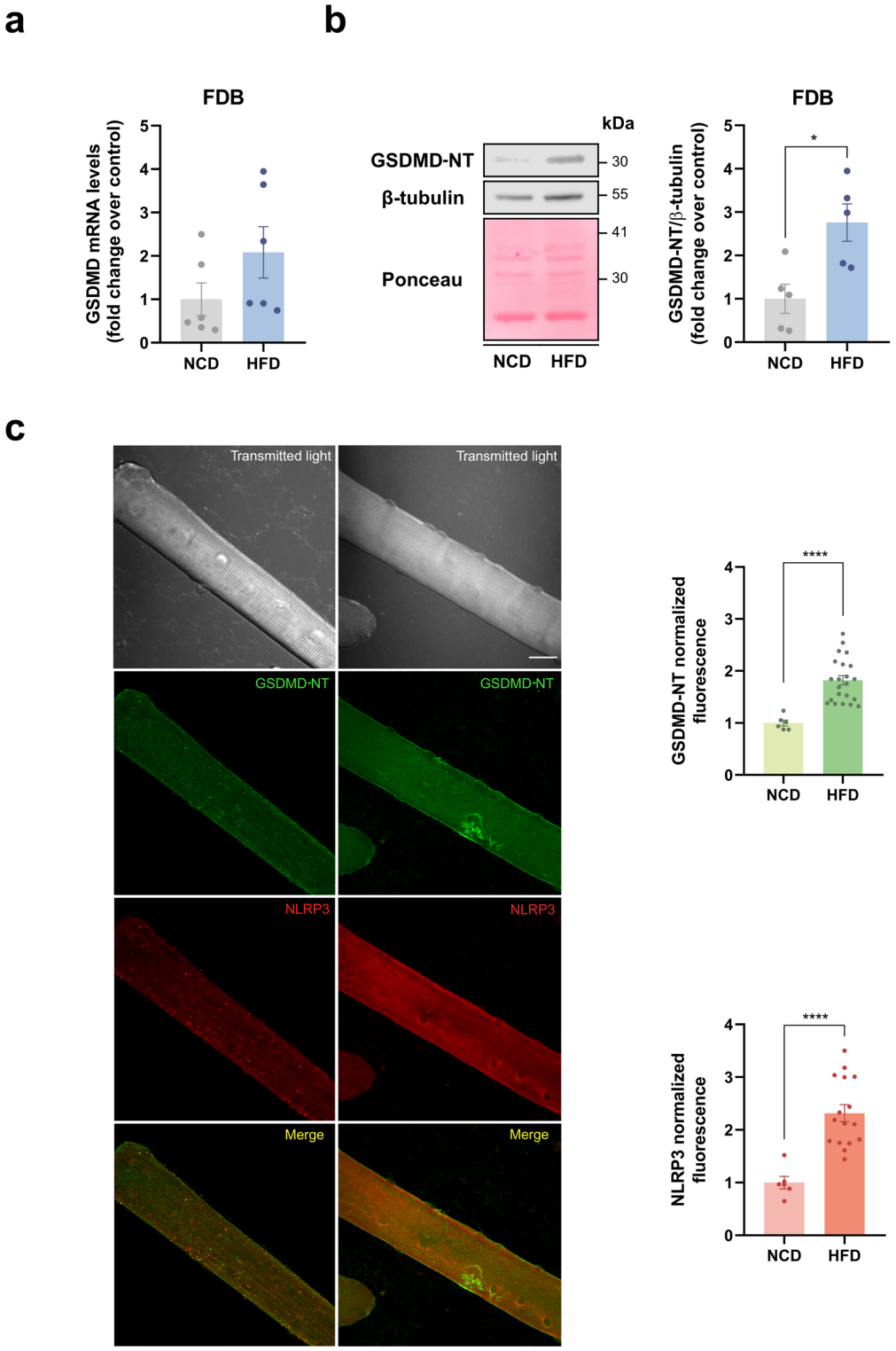

Fig. 1. High-fat diet feeding increases protein levels of GSDMD-NT in the FDB muscle of insulin-resistant mice. **a** Relative mRNA levels of GSDMD in isolated adult fibers quantified by RT-qPCR and normalized to the housekeeping gene RplpO (n = 6). **b** Representative Western blot and densitometric quantification of GSDMD-NT protein levels in muscle homogenates (n = 5). β-tubulin was used as a loading control. **c** Representative confocal microscopy images of isolated FDB fibers from the NCD and HFD groups, illustrating the localization of GSDMD-NT (green) and NLRP3 (red), along with the quantification of the average fluorescence intensity of GSDMD-NT and NLRP3 in both groups (n = 3 independent experiments). Scale bar = 40 µm. Results are presented as mean ± SEM and expressed relative to the NCD group. The data were analyzed using the Mann-Whitney *U* test for statistical evaluation. $^{*}p < 0.05$ and $^{****}p < 0.0001$ vs NCD. NCD: normal-control diet; HFD: high-fat diet; FDB: flexor digitorum brevis.

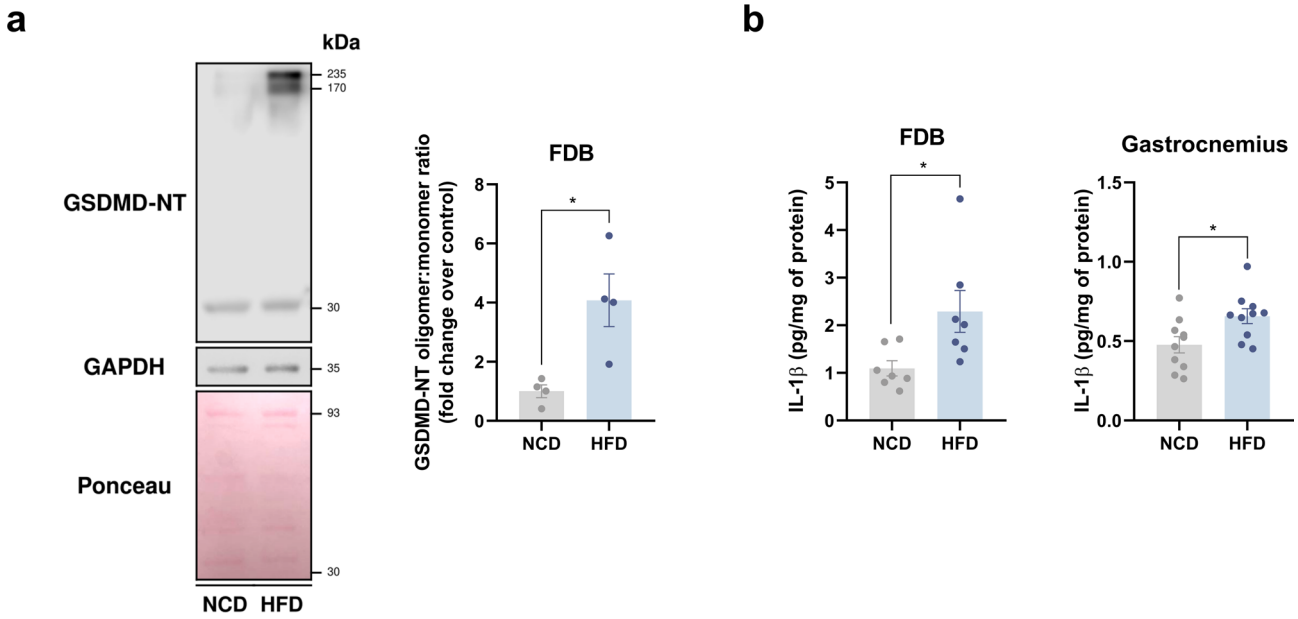

Fig. 2. A high-fat diet enhances GSDMD-NT oligomerization and promotes IL-1β release in the skeletal muscle of insulin-resistant mice. **a** Representative Western blot assay and quantification of the oligomer:monomer ratio of GSDMD-NT in non-reducing gels from FDB muscle (n = 4). **b** IL-1β release levels were measured in the culture medium of FDB (n = 7) and gastrocnemius (n = 10), respectively, and expressed as pg/mg of protein. Data are presented as mean ± SEM and expressed relative to values from the NCD group. The data were analyzed using the Mann-Whitney *U* test for statistical analysis.*$p < 0.05$ vs NCD. NCD: normal-control diet; HFD: high-fat diet; FDB: flexor digitorum brevis.

improvement in the IPGTT ($p < 0.0001$) with an AUG of 27,197 ± 1,076 (mg·min/dL) and 36,240 ± 838 (mg·min/dL), respectively (Fig. 3a-d). Additionally, IL-1β plasma levels (Fig. 3d) were also diminished ($p = 0.041$) in DSF-treated mice (3.08 ± 0.17 pg/mL) compared to vehicle-treated mice (4.65 ± 0.53 pg/mL). These results suggest that DSF reduces glucose levels in obesity-induced IR mice after three weeks of treatment.

Disulfiram increases insulin-dependent Akt phosphorylation and glucose uptake in skeletal muscle

To determine whether DSF modulates insulin signaling activation, we assessed Akt phosphorylation at serine 473 (S473) in whole-muscle homogenates from FDB using Western blot analysis (Fig. 4a). As expected, in HFD-fed mice, insulin pre-incubation did not alter Akt phosphorylation at S473 ($p = 0.583$) in vehicle-treated mice compared to basal conditions (2.02 ± 0.13-fold vs. 1.00 ± 0.07-fold, respectively). In contrast, DSF-treated HFD-fed mice show an increase in insulin-stimulated Akt phosphorylation at S473 ($p = 0.031$), reaching 4.14 ± 0.89-fold compared to their basal levels (1.60 ± 0.65-fold). To further assess this point, glucose uptake was determined by measuring 2-NBDG incorporation, a fluorescent glucose analogue. As shown in Fig. 4b, insulin increased 2-NBDG uptake in fibers isolated from DSF-treated HFD-fed mice, from 1.25 ± 0.01-fold under basal conditions to 1.45 ± 0.01-fold with insulin stimulation ($p = 0.047$). Conversely, fibers from vehicle-injected mice showed a 2-NBDG uptake of 1.00 ± 0.08-fold in basal conditions and 1.17 ± 0.05-fold after insulin stimulation ($p = 0.091$). Moreover, insulin-stimulated 2-NBDG uptake was higher in muscle fibers from DSF-treated HFD-fed mice than in those from vehicle-treated mice ($p = 0.006$). To evaluate the effect of DSF on GLUT4 translocation, we analyzed the fluorescence pattern of GLUT4-7*myc*-eGFP in isolated adult FDB muscle fibers from HFD-fed mice preincubated with 10 nM DSF or vehicle (DMSO) for 24 h. Representative confocal images of fibers illustrate the effects of insulin on GLUT4-7*myc*-eGFP translocation (Fig. Suppl. 7). Consistent with glucose uptake data, stimulation with 100 nM insulin did not promote a significant increase in GLUT4-7*myc*-eGFP membrane translocation (1.59 ± 0.30-fold) compared with fibers under basal conditions isolated from HFD-fed mice (1.00 ± 0.14-fold). In contrast, 10 nM DSF for 24 h increased insulin-stimulated GLUT4-7*myc*-eGFP translocation to the plasma membrane (3.45 ± 0.64-fold; $p = 0.008$), suggesting an improvement of insulin responsiveness in skeletal muscle fibers from HFD-fed mice.

Disulfiram reduces GSDMD-NT oligomerization and IL-1β release in skeletal muscle from HFD-fed mice

To assess whether DSF modulates the inflammatory processes, we performed Western blot and ELISA in the whole skeletal muscle. In both experiments, skeletal muscle was incubated with 10 nM DSF for 24 h. This treatment significantly reduced ($p = 0.029$) the GSDMD-NT oligomer-to-monomer ratio in the gastrocnemius muscle of HFD-fed mice, reaching values of 0.49 ± 0.06-fold compared to 1.00 ± 0.21-fold in DMSO-treated muscle (Fig. 5a). Accordingly, IL-1β release from ex vivo skeletal muscle was also diminished ($p = 0.028$)

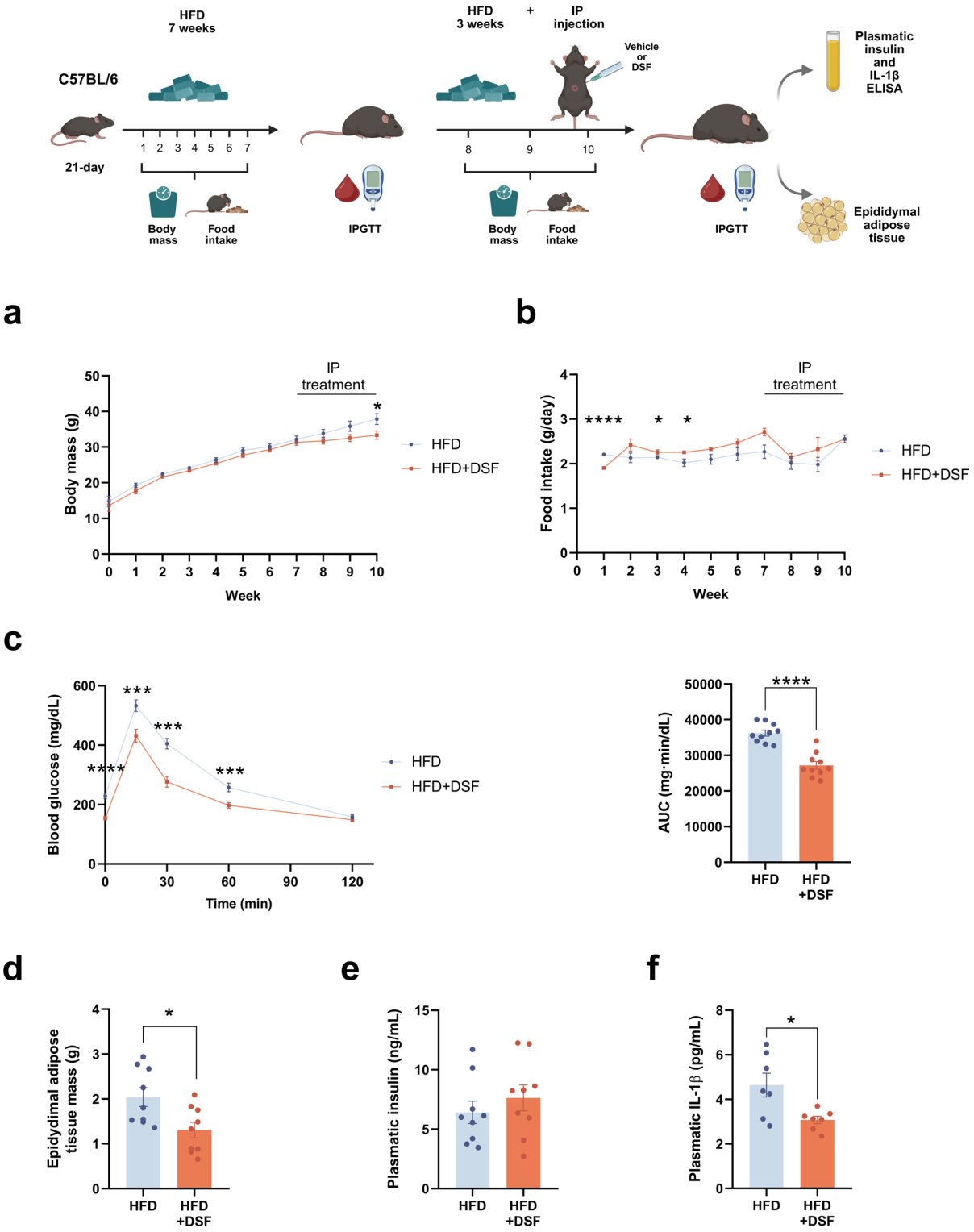

Fig. 3. Disulfiram administration improves physiological parameters in obese insulin-resistant mice. HFD-fed 7-week-old mice were intraperitoneally injected with DSF 50 mg/kg or vehicle three times per week for 3 weeks. **a** Body mass progression (n = 10). **b** Weekly variation in food intake (n = 10). **c** Intraperitoneal glucose tolerance test (IPGTT) and its area under the curve (AUC). (n = 10). **d** Epididymal adipose tissue mass (n = 9). **e** Fasting insulinemia (n = 9). **f** Plasma IL-1β levels in HFD-fed mice (n = 7). Results are presented as mean ± SEM and expressed relative to the HFD group.*$p < 0.05$, ***$p < 0.001$, and ****$p < 0.0001$ vs. HFD. HFD: High-fat diet, HFD DSF: High-fat diet injected with disulfiram, FDB: flexor digitorum brevis.

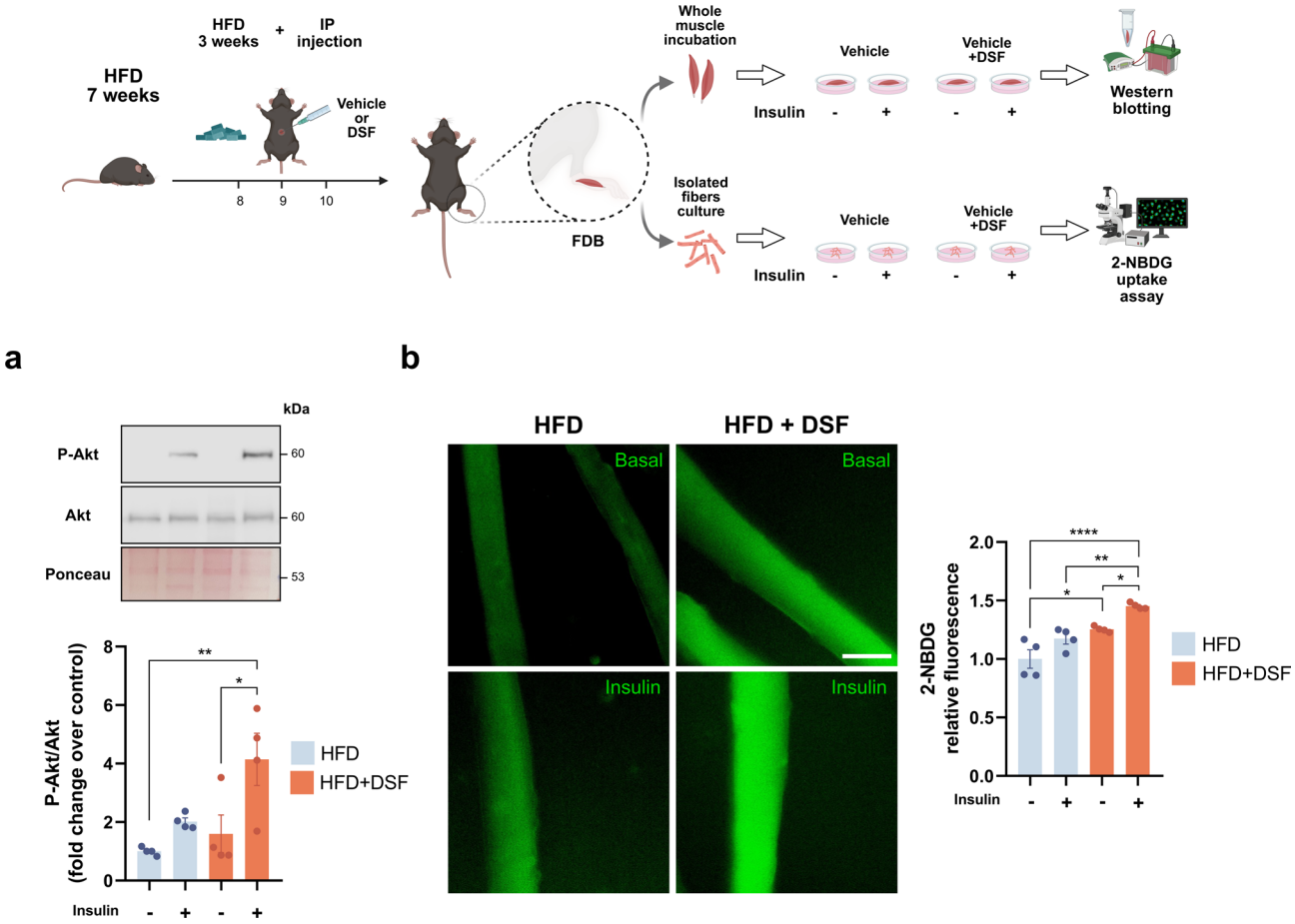

Fig. 4. Disulfiram promotes insulin-dependent Akt phosphorylation and increases glucose uptake in FDB muscle fibers in insulin-resistant mice. Ratio of phosphorylated to total Akt (P-Akt/Akt) in FDB and 2-NBDG uptake assay in FDB muscle fibers. **a** Representative Western blot assay and quantification of P-Akt protein levels in muscle homogenates (n = 4). Total Akt was used as a loading control. **b** Representative epifluorescence images (green fluorescence) and quantification of 2-NBDG uptake (n = 4 independent experiments). 2-NBDG was used at 300 µM; insulin at 100 nM for 20 minutes. (Scale bar = 50 µm). For the analysis of four groups, a two-way ANOVA with Tukey's multiple comparisons test was performed. Results are presented as mean ± SEM and expressed relative to the HFD group. * $p < 0.05$, ** $p < 0.01$, and **** $p < 0.0001$ vs. HFD. HFD: High-fat diet, HFD+DSF: High-fat diet injected with 50 mg/kg three times per week for 3 weeks. FDB: flexor digitorum brevis.

following DSF incubation (0.46 ± 0.03 pg/mg) compared to DMSO-treated muscle (0.72 ± 0.16 pg/mg) (Fig. 5b). These findings suggest that DSF inhibits IL-1β release through reduction of GSDMD-NT oligomerization in skeletal muscle under metabolic stress conditions. Next, to assess whether DSF inhibits NLRP3 inflammasome activation, caspase-1 activity was assessed in isolated skeletal muscle fibers from HFD-fed mice (Fig. Suppl. 8). Incubation with 10 nM DSF for 24 h significantly reduced caspase-1 activity in fibers from HFD-fed mice compared with vehicle ($p = 0.007$), indicating that DSF suppresses NLRP3 inflammasome activation in skeletal muscle (Fig. Suppl. 8a). In addition, intracellular levels of IL-1β exhibited an increase after injection with DSF ($p < 0.001$) (Fig. Suppl. 8b). This pattern is also observed as a tendency in response of incubation with 10 nM DSF for 24 h, suggesting that DSF may prevent IL-1β release from skeletal muscle fibers. (Fig. Suppl. 8c). Altogether, these findings suggest that DSF may inhibit not only GSDMD-NT oligomerization but also NLRP3 inflammasome activation, thereby preventing IL-1β release from skeletal muscle fibers.

Discussion

Chronic low-grade inflammation contributes to the pathogenesis of IR during obesity[25–27]. NLRP3 activation plays a main role in this response, primarily mediated by immune cells[8]. Nevertheless, its expression and activation have also been demonstrated in non-immune tissues, including human adipocytes[28], hepatocytes[29], and skeletal muscle[9]. We previously showed that NLRP3 inflammasome activation inhibits GLUT4 translocation and disrupts insulin signaling in skeletal muscle[9,30]. These findings align with NLRP3-mediated inflammatory activity linked to metabolic dysfunction in skeletal muscle[31]. In this study, we determined that GSDMD contributes to IL-1β release and could disrupt glucose homeostasis in skeletal muscle under NLRP3-mediated metabolic

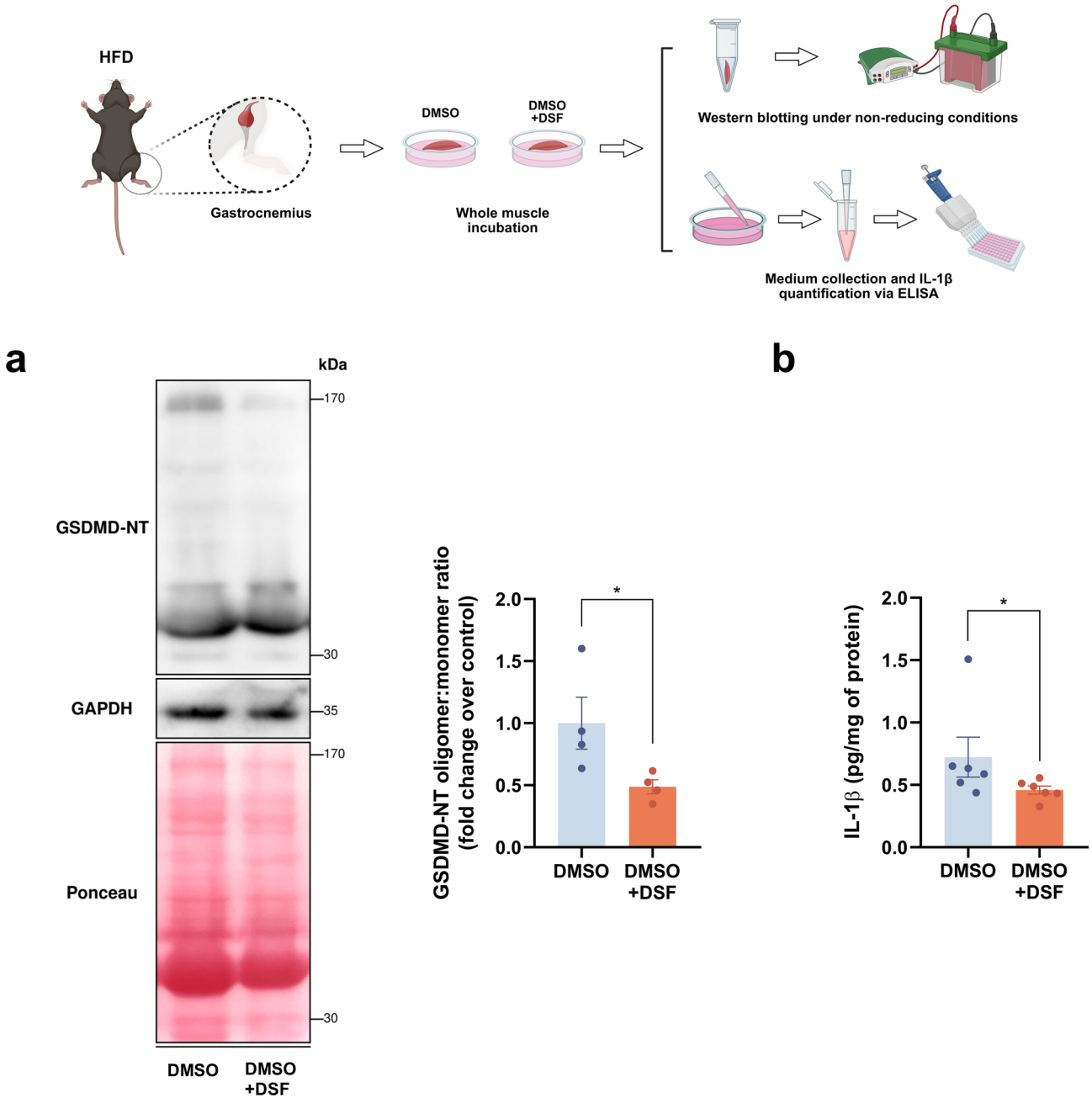

Fig. 5. Disulfiram administration reduces GSDMD-NT oligomerization and IL-1β release from the gastrocnemius muscle of mice fed a high-fat diet. **a** Representative Western blot assay and quantification of the oligomer/monomer ratio of GSDMD-NT in non-reducing gels (n = 4). **b** IL-1β release levels were measured in the culture medium (n = 6) and expressed as pg/mg of protein. Values are presented as the mean ± SEM and expressed relative to the HFD condition incubated with DMSO. The data were analyzed using the Mann-Whitney *U* test for statistical evaluation. **p* < 0.05 vs HFD. HFD: high-fat diet, DMSO: Dimethyl sulfoxide, DSF: Disulfiram at a concentration of 10 nM.

inflammation. Moreover, DSF treatment mitigates these alterations by reducing GSDMD-NT oligomerization, pore formation and IL-1β release, supporting GSDMD as a potential target to attenuate metabolic inflammation and improve glucose handling in obesity-induced IR.

In HFD-fed mice, GSDMD-NT protein levels were increased and localized primarily to the sarcolemma and T-tubules in skeletal muscle. This spatial distribution may be particularly relevant for facilitating IL-1β release, promoting a local positive feedback loop that sustains NLRP3 inflammasome activation and drives chronic inflammation, contributing to metabolic dysfunction and IR (Figs. 1 and 2). The detection of oligomers within the 170–235 kDa range supports the hypothesis of an active pore formation in sarcolemma and T-tubule without reducing fiber viability. Approximately 6–8 GSDMD-NT molecules oligomerize to form a pore in FDB skeletal

muscle fibers (Fig. 2a), a stoichiometry lower than that reported in previous studies using atomic force microscopy, which have shown GSDMD-NT pores composed of 18 to 36 subunits[32]. Although GSDMD-NT oligomerization is associated with pyroptosis, it has been suggested that IL-1β can be released through sublytic pores without causing complete membrane rupture in macrophages, dendritic cells, and partially in neutrophils[13]. Recent studies have demonstrated that small oligomers, such as pentamers, can form stable pores exhibiting sublytic activity with limited membrane disruption[33]. Although the precise mechanism of pore formation remains unclear, cysteine residues are emerging as key modulators of the oligomerization process. Notably, Cys39, Cys57, and particularly Cys191/192 (Cys191 in humans; Cys192 in mice) have been identified as key mediators of this process[34]. In the context of IR, oxidative stress is known to activate the NLRP3 inflammasome via interaction with thioredoxin-interacting protein (TXNIP) in skeletal muscle[30]. Reactive oxygen species (ROS) have also been shown to promote GSDMD-NT oligomerization, with Cys192 being essential for ROS sensitivity[35]. Moreover, the S-palmitoylation of Cys192 has been implicated in regulating GSDMD membrane targeting[34]. Nevertheless, whether these or other cysteine residues contribute specifically to GSDMD-NT oligomerization in skeletal muscle remains to be determined.

It is well-established that skeletal muscle is active in secreting inflammatory factors and bioactive peptides, known as myokines, under normal or IR conditions[36,37]. We observed increased IL-1β levels in the culture media of FDB and gastrocnemius muscles from IR mice, suggesting the contribution of skeletal muscle tissue to the inflammation associated with this metabolic dysfunction. IL-1β is secreted through several non-classical mechanisms, including lysosomal exocytosis, microvesicle shedding, fusion of multivesicular bodies and exosomes, GSDMD-NT pore formation, and passive release following cell lysis[38]. Our results show elevated GSDMD-NT oligomerization in skeletal muscle fibers (Fig. 2b), suggesting that IL-1β may be exported through GSDMD-formed pores, contributing to local signaling events that could impair insulin sensitivity[39]. Due to its half-life in plasma (19.0 min in rats), IL-1β-associated vesicles and/or exosomes may mediate effects in distant sites rather than only at the local inflammatory tissue[40]. In this context, the reduction in NLRP3 inflammasome activation and subsequent IL-1β release could limit proinflammatory signaling, thereby improving metabolic homeostasis in obesity-induced insulin-resistant mice.

DSF, originally approved for the treatment of chronic alcohol dependence, exhibits a well-established safety profile in adherent patients, and long-term administration has not been associated with the development of pharmacological tolerance[15]. DSF covalently modifies a conserved cysteine residue Cys191/192 in GSDMD, inhibiting pore formation and pyroptosis[14]. Recently, prolonged DSF treatment for 40 to 60 weeks in obese mice has been reported to normalize body weight, improve fasting glycemia, reduce adiposity, and restore systemic insulin responsiveness[16]. However, its potential effects on insulin sensitivity in skeletal muscle had not been previously explored. The present findings suggest that a short-term DSF treatment lasting three weeks reduced body weight in HFD-induced obese mice without altering food intake (Fig. 3). These results indicate that, at the examined time point, DSF exerts tissue-specific effects rather than through modulation of feeding behavior. This finding is consistent with previous reports indicating a weight-lowering effect of DSF[16] and extends them by demonstrating its efficacy over a shorter intervention period. The absence of changes in dietary intake suggests that DSF may modulate mechanisms of energy expenditure or metabolic efficiency[41,42]. In DSF-treated HFD-obese mice, we observed a decrease in IPGTT and fasting blood glucose with reduced plasma IL-1β concentrations, suggesting a link between improved glucose homeostasis and attenuation of inflammation. Moreover, DSF-treated mice exhibit improved glycemic control in response to insulin, consistent with previous reports for long-term treatment[16,43,44]. Our results provide new evidence supporting the notion that short-term DSF treatment enhances insulin sensitivity in skeletal muscle under obesity-induced IR, showing a new aspect of its metabolic effects.

Consistent with improved insulin responsiveness, DSF treatment increased insulin-stimulated phosphorylation of Akt at S473 in skeletal muscle from HFD-fed mice (Fig. 4a), indicating enhanced insulin signaling downstream of the insulin receptor. In concordance, DSF-treated HFD-fed mice also exhibit improved insulin-stimulated glucose uptake (Fig. 4b), consistent with a functional increase in glucose disposal. These results suggest that DSF may affect insulin signaling pathways in skeletal muscle and contribute to improved peripheral glucose utilization[42]. Nevertheless, skeletal muscle also expresses GLUT1, an insulin-independent glucose transporter with constitutive activity[45]. Interestingly, glucose uptake was also increased in fiber from DSF-treated HFD mice, even in the absence of exogenous insulin stimulation, suggesting that DSF may increase basal glucose transport through insulin-independent mechanisms. Recently, it has been reported that DSF exerts insulin-independent and insulin-sensitizing effects without reversing palmitate-induced insulin resistance as determined by GLUT4-HA translocation in L6 myotubes[46]. In our study, however, DSF treatment increased insulin-stimulated GLUT4 translocation in skeletal muscle fibers isolated from HFD-fed mice (Fig. Suppl. 7). This apparent discrepancy suggests that the insulin-sensitizing effect of DSF may be influenced by the metabolic context or the cellular model employed. Specifically, DSF appears to improve insulin responsiveness in insulin-resistant skeletal muscle fibers, whereas its effect is not evident in myotubes expose to acute lipotoxic stress induced by palmitate[46]. Such differences may reflect distinct mechanisms of insulin resistance and cellular adaptations operating in in vivo–derived muscle fibers compared to cultured myotubes.

Furthermore, we found that DSF reduced GSDMD-NT oligomerization and IL-1β release from the gastrocnemius muscle from HFD-fed mice (Fig. 5). Previous studies have shown that a HFD increases the release of other pro-inflammatory cytokines, such as IL-6 and TNF-α, from skeletal muscle fibers, and elevates their plasma concentrations[47]. Notably, these cytokines are not reduced by DSF treatment[16], suggesting that the modulatory effect of DSF may be relatively specific to IL-1β release rather than broadly targeting multiple cytokines. Interestingly, DSF reduced caspase-1 activity while concomitantly increasing intracellular IL-1β levels (Fig. Suppl. 8). These results suggest that DSF-mediated inhibition of GSDMD-NT reduces IL-1β release, thereby limiting a possible autocrine and/or paracrine signaling in skeletal muscle and contributing to decreased NLRP3

inflammasome activation, as evidenced by lower caspase-1 activity in muscle fibers (Fig. Suppl. 8). In line with this interpretation, it has been recently reported that DSF inhibits the palmitoylation of the NLRP3 protein at Cys126, a post-translational modification required for its activation[48]. Although our study was not specifically designed to address this mechanism, we cannot rule out that DSF-mediated inhibition of NLRP3 palmitoylation may also contribute to the reduction in inflammasome activity observed in skeletal muscle from HFD-fed mice. These findings suggest that DSF exerts anti-inflammatory effects through the modulation of NLRP3-related pathways, which may contribute to its overall metabolic improvements observed in skeletal muscle. However, we cannot rule out an effect of DSF in another tissues. Treatment of obese mice with DSF prevented weight gain and improved insulin responsiveness while reducing liver, pancreatic, and adipose abnormalities associated with high-fat diets. These metabolic benefits were accompanied by decreased low-grade inflammation and improved insulin secretion, suggesting that DSF can both prevent and reverse obesity-associated insulin resistance[16]. Consistent with our findings, DSF was shown to counteract skeletal muscle atrophy and insulin resistance in mice by modulating the Sirt2 pathway and inhibiting the NLRP3/caspase-1/GSDMD inflammatory axis[49]. These results reinforce the notion that the anti-inflammatory effects of DSF in skeletal muscle involve specific molecular mechanisms that regulate cytokine release such as IL-1β, ultimately preserving muscle integrity and improving insulin sensitivity. Thus, chronic inflammation in skeletal muscle, often driven by obesity, disrupts insulin signaling and glucose uptake, thereby promoting systemic insulin resistance[49]. Muscle-derived signaling molecules, or myokines, can either exacerbate or alleviate this condition, underscoring the central role of muscle inflammation in metabolic health[50].

In this context, repurposing DSF as an anti-inflammatory agent represents a promising therapeutic strategy[43], particularly in metabolic diseases where chronic skeletal muscle inflammation plays a central role. While previous studies have explored the potential role of DSF in metabolic regulation on glucose in diabetic animal models[16], the evidence in humans with type 2 diabetes remains very limited. Importantly, an observational study reported that DSF administration was associated with an increased risk of hypoglycemia-related hospitalization, with an odds ratio of 4.21 (95% CI 2.05–8.62)[51]. These findings suggest that DSF may play a role in the regulation of glucose uptake. However, its potential clinical application in treatment of diabetes and other related complications should be approached with caution, and further well-designed human studies are needed to confirm its safety and efficacy.

Conclusion

In conclusion, our study identifies GSDMD-NT–mediated IL-1β release as a possible driver of skeletal muscle insulin resistance. By inhibiting both GSDMD-NT oligomerization and NLRP3 inflammasome, DSF could attenuate inflammatory signaling, reduces IL-1β release, and improves insulin responsiveness and glucose disposal. These findings position GSDMD-NT as a potential mechanistic link between inflammation and metabolic dysfunction, and highlight DSF as a promising therapeutic candidate for obesity-associated insulin resistance and type 2 diabetes. Future clinical investigations should be conducted with caution to validate the efficacy and confirm the safety of DSF, as well as to define its potential therapeutic application in human metabolic disorders.

Limitations

This study provides experimental evidence suggesting a role for GSDMD-NT in skeletal muscle inflammation and insulin resistance. It shows that pharmacological inhibition with DSF improves glucose homeostasis in a diet-induced obesity model. However, some limitations should be acknowledged. First, although our results support a functional effect of DSF on insulin signaling, the study was not designed to investigate molecular targets beyond GSDMD-NT and caspase-1. Second, our data indicate metabolic benefits in skeletal muscle from short-term DSF treatment; however, its long-term effects and translational relevance remain to be explored in future studies. Third, in the present study, we did not have access to genetic models, limiting our ability to directly determine the contribution of GSDMD to skeletal muscle inflammation and insulin resistance. Although our data indicate that GSDMD activation is associated with IL-1β release and impaired insulin signaling, future studies using *Gsdmd-/-* mice or muscle-specific *Gsdmd* knockdown approaches will be required to establish a causal relationship and to confirm that the effects of DSF are mediated through GSDMD inhibition.

Data availability

The datasets and/or analyses during the current study are available from the corresponding author on reasonable request.

Received: 14 July 2025; Accepted: 20 November 2025
Published online: 26 November 2025

References

1. Saeedi, P. et al. Global and regional diabetes prevalence estimates for 2019 and projections for 2030 and 2045: results from the international diabetes federation diabetes Atlas, 9th edition. *Diabetes Res. Clin. Pract.* **157**, 107843. https://doi.org/10.1016/j.diabres.2019.107843 (2019).
2. James, D. E., Stöckli, J. & Birnbaum, M. J. The aetiology and molecular landscape of insulin resistance. *Nat. Rev. Mol. Cell. Biol.* **22** (11), 751–771. https://doi.org/10.1038/s41580-021-00390-6 (2021).
3. Kim, M. S. et al. Association of genetic risk, lifestyle, and their interaction with obesity and obesity-related morbidities. *Cell. Metab.* **36** (7), 1494–1503e3. https://doi.org/10.1016/j.cmet.2024.06.004 (2024).

4. DeFronzo, R. A., Gunnarsson, R., Björkman, O., Olsson, M. & Wahren, J. Effects of insulin on peripheral and splanchnic glucose metabolism in noninsulin-dependent (type II) diabetes mellitus. *J. Clin. Invest.* **76** (1), 149–155. https://doi.org/10.1172/JCI111938 (1985).
5. Saltiel, A. R. & Olefsky, J. M. Inflammatory mechanisms linking obesity and metabolic disease. *J. Clin. Invest.* **127** (1), 1–4. https://doi.org/10.1172/JCI92035 (2017).
6. Rohm, T. V., Meier, D. T., Olefsky, J. M. & Donath, M. Y. Inflammation in obesity, diabetes, and related disorders. *Immunity* **55** (1), 31–55. https://doi.org/10.1016/j.immuni.2021.12.013 (2022).
7. Kelley, N., Jeltema, D., Duan, Y. & He, Y. The NLRP3 inflammasome: an overview of mechanisms of activation and regulation. *Int. J. Mol. Sci.* **20** (13), 3328. https://doi.org/10.3390/ijms20133328 (2019).
8. Rheinheimer, J., de Souza, B. M., Cardoso, N. S., Bauer, A. C. & Crispim, D. Current role of the NLRP3 inflammasome on obesity and insulin resistance: A systematic review. *Metabolism* **74**, 1–9. https://doi.org/10.1016/j.metabol.2017.06.002 (2017).
9. Américo-Da-Silva, L. et al. Activation of the NLRP3 inflammasome increases the IL-1β level and decreases GLUT4 translocation in skeletal muscle during insulin resistance. *Int. J. Mol. Sci.* **22** (19), 10212. https://doi.org/10.3390/ijms221910212 (2021).
10. Lieberman, J., Wu, H. & Kagan, J. C. Gasdermin D activity in inflammation and host defense. *Sci. Immunol.* **4** (39), eaav1447. https://doi.org/10.1126/sciimmunol.aav1447 (2019).
11. Yang, J. et al. Mechanism of gasdermin D recognition by inflammatory caspases and their Inhibition by a gasdermin D-derived peptide inhibitor. *Proc. Natl. Acad. Sci. U S A.* **115** (26), 6792–6797. https://doi.org/10.1073/pnas.1800562115 (2018).
12. Kuang, S. et al. Structure insight of GSDMD reveals the basis of GSDMD autoinhibition in cell pyroptosis. *Proc. Natl. Acad. Sci. U S A.* **114** (40), 10642–10647. https://doi.org/10.1073/pnas.1708194114 (2017).
13. Heilig, R. et al. The Gasdermin-D pore acts as a conduit for IL-1β secretion in mice. *Eur. J. Immunol.* **48** (4), 584–592. https://doi.org/10.1002/eji.201747404 (2018).
14. Hu, J. J. et al. FDA-approved Disulfiram inhibits pyroptosis by blocking gasdermin D pore formation. *Nat. Immunol.* **21** (7), 736–745. https://doi.org/10.1038/s41590-020-0669-6 (2020).
15. Fuller, R. K. et al. Disulfiram treatment of alcoholism. A veterans administration cooperative study. *JAMA* **256** (11), 1449–1455 (1986).
16. Bernier, M. et al. Disulfiram treatment normalizes body weight in obese mice. *Cell. Metab.* **32** (2), 203–214e4. https://doi.org/10.1016/j.cmet.2020.04.019 (2020).
17. Bernier, M. et al. Elucidating the mechanisms by which Disulfiram protects against obesity and metabolic syndrome. *NPJ Aging Mech. Dis.* **6**, 8. https://doi.org/10.1038/s41514-020-0046-6 (2020).
18. Sánchez-Aguilera, P. et al. Role of ABCA1 on membrane cholesterol content, insulin-dependent Akt phosphorylation and glucose uptake in adult skeletal muscle fibers from mice. *Biochim. Biophys. Acta Mol. Cell. Biol. Lipids.* **1863** (12), 1469–1477. https://doi.org/10.1016/j.bbalip.2018.09.005 (2018).
19. DiFranco, M., Quinonez, M., Capote, J. & Vergara, J. DNA transfection of mammalian skeletal muscles using in vivo electroporation. *J. Vis. Exp. JoVE.* (32), 1520. https://doi.org/10.3791/1520 (2009).
20. Llanos, P. et al. The cholesterol-lowering agent methyl-β-cyclodextrin promotes glucose uptake via GLUT4 in adult muscle fibers and reduces insulin resistance in obese mice. *Am. J. Physiol. Endocrinol. Metab.* **308** (4), E294–305. https://doi.org/10.1152/ajpendo.00189.2014 (2015).
21. Jaldin-Fincati, J. R., Bilan, P. J. & Klip, A. GLUT4 translocation in single muscle cells in culture: epitope detection by Immunofluorescence. *Methods Mol. Biol. Clifton NJ.* **1713**, 175–192. https://doi.org/10.1007/978-1-4939-7507-5_14 (2018).
22. Knudsen, J. R., Henriquez-Olguin, C., Li, Z. & Jensen, T. E. Electroporated GLUT4-7myc-GFP detects in vivo glucose transporter 4 translocation in skeletal muscle without discernible changes in GFP patterns. *Exp. Physiol.* **104** (5), 704–714. https://doi.org/10.1113/EP087545 (2019).
23. Hidalgo, C., Jorquera, J., Tapia, V. & Donoso, P. Triads and transverse tubules isolated from skeletal muscle contain high levels of inositol 1,4,5-trisphosphate. *J. Biol. Chem.* **268** (20), 15111–15117 (1993).
24. Evavold, C. L. et al. The Pore-Forming protein gasdermin D regulates Interleukin-1 secretion from living macrophages. *Immunity* **48** (1), 35–44e6. https://doi.org/10.1016/j.immuni.2017.11.013 (2018).
25. Shoelson, S. E., Lee, J. & Goldfine, A. B. Inflammation and insulin resistance. *J. Clin. Invest.* **116** (7), 1793–1801. https://doi.org/10.1172/JCI29069 (2006).
26. Ellulu, M. S., Patimah, I., Khaza'ai, H., Rahmat, A. & Abed, Y. Obesity and inflammation: the linking mechanism and the complications. *Arch. Med. Sci. AMS.* **13** (4), 851–863. https://doi.org/10.5114/aoms.2016.58928 (2017).
27. Soták, M., Clark, M., Suur, B. E. & Börgeson, E. Inflammation and resolution in obesity. *Nat. Rev. Endocrinol.* **21** (1), 45–61. https://doi.org/10.1038/s41574-024-01047-y (2025).
28. D'Espessailles, A., Mora, Y. A., Fuentes, C. & Cifuentes, M. Calcium-sensing receptor activates the NLRP3 inflammasome in LS14 preadipocytes mediated by ERK1/2 signaling. *J. Cell. Physiol.* **233** (8), 6232–6240. https://doi.org/10.1002/jcp.26490 (2018).
29. Csak, T. et al. Fatty acid and endotoxin activate inflammasomes in mouse hepatocytes that release danger signals to stimulate immune cells. *Hepatol. Baltim. Md.* **54** (1), 133–144. https://doi.org/10.1002/hep.24341 (2011).
30. Russell-Guzmán, J. et al. Activation of the ROS/TXNIP/NLRP3 pathway disrupts insulin-dependent glucose uptake in skeletal muscle of insulin-resistant obese mice. *Free Radic Biol. Med.* **222**, 187–198. https://doi.org/10.1016/j.freeradbiomed.2024.06.011 (2024).
31. Vandanmagsar, B. et al. The NLRP3 inflammasome instigates obesity-induced inflammation and insulin resistance. *Nat. Med.* **17** (2), 179–188. https://doi.org/10.1038/nm.2279 (2011).
32. Mari, S. A. et al. Gasdermin-A3 pore formation propagates along variable pathways. *Nat. Commun.* **13** (1), 2609. https://doi.org/10.1038/s41467-022-30232-8 (2022).
33. Schaefer, S. L. & Hummer, G. Sublytic gasdermin-D pores captured in atomistic molecular simulations. *eLife* **11**, e81432. https://doi.org/10.7554/eLife.81432 (2022).
34. Margheritis, E. et al. Gasdermin D cysteine residues synergistically control its palmitoylation-mediated membrane targeting and assembly. *EMBO J.* **43** (19), 4274–4297. https://doi.org/10.1038/s44318-024-00190-6 (2024).
35. Devant, P. et al. Gasdermin D pore-forming activity is redox-sensitive. *Cell. Rep.* **42** (1), 112008. https://doi.org/10.1016/j.celrep.2023.112008 (2023).
36. Merz, K. E. & Thurmond, D. C. Role of skeletal muscle in insulin resistance and glucose uptake. *Compr. Physiol.* **10** (3), 785–809. https://doi.org/10.1002/cphy.c190029 (2020).
37. Pedersen, B. K. & Febbraio, M. A. Muscles, exercise and obesity: skeletal muscle as a secretory organ. *Nat. Rev. Endocrinol.* **8** (8), 457–465. https://doi.org/10.1038/nrendo.2012.49 (2012).
38. Artlett, C. M. The role of the NLRP3 inflammasome in fibrosis. *Open. Rheumatol. J.* **6**, 80–86. https://doi.org/10.2174/1874312901206010080 (2012).
39. Jorquera, G. et al. NLRP3 inflammasome: potential role in obesity related Low-Grade inflammation and insulin resistance in skeletal muscle. *Int. J. Mol. Sci.* **22** (6), 3254. https://doi.org/10.3390/ijms22063254 (2021).
40. Kudo, S., Mizuno, K., Hirai, Y. & Shimizu, T. Clearance and tissue distribution of Recombinant human Interleukin 1 beta in rats. *Cancer Res.* **50** (18), 5751–5755 (1990).
41. Gill, R. M., O'Brien, M., Young, A., Gardiner, D. & Mailloux, R. J. Protein S-glutathionylation lowers superoxide/hydrogen peroxide release from skeletal muscle mitochondria through modification of complex I and Inhibition of pyruvate uptake. *PloS One.* **13** (2), e0192801. https://doi.org/10.1371/journal.pone.0192801 (2018).

42. Hirschenson, J. & Mailloux, R. J. The glutathionylation agent Disulfiram augments superoxide/hydrogen peroxide production when liver mitochondria are oxidizing ubiquinone pool-linked and branched chain amino acid substrates. *Free Radic Biol. Med.* **172**, 1–8. https://doi.org/10.1016/j.freeradbiomed.2021.05.030 (2021).
43. Omran, Z., Sheikh, R., Baothman, O. A., Zamzami, M. A. & Alarjah, M. Repurposing Disulfiram as an Anti-Obesity drug: treating and preventing obesity in High-Fat-Fed rats. *Diabetes Metab. Syndr. Obes. Targets Ther.* **13**, 1473–1480. https://doi.org/10.2147/DMSO.S254267 (2020).
44. Nagai, N., Murao, T., Okamoto, N. & Ito, Y. Disulfiram reduces elevated blood glucose levels in Otsuka Long-Evans Tokushima fatty (OLETF) rats, a model of type 2 diabetes. *J. Oleo Sci.* **58** (9), 485–490. https://doi.org/10.5650/jos.58.485 (2009).
45. Jones, J. P., Tapscott, E. B., Olson, A. L., Pessin, J. E. & Dohm, G. L. Regulation of glucose transporters GLUT-4 and GLUT-1 gene transcription in denervated skeletal muscle. *J. Appl. Physiol. Bethesda Md. 1985.* **84** (5), 1661–1666. https://doi.org/10.1152/jappl.1998.84.5.1661 (1998).
46. Masson, S. W. C. et al. Leveraging genetic diversity to identify small molecules that reverse mouse skeletal muscle insulin resistance. *eLife* **12**, RP86961. https://doi.org/10.7554/eLife.86961 (2023).
47. Jorquera, G. et al. High extracellular ATP levels released through pannexin-1 channels mediate inflammation and insulin resistance in skeletal muscle fibres of diet-induced obese mice. *Diabetologia* **64** (6), 1389–1401. https://doi.org/10.1007/s00125-021-05418-2 (2021).
48. Xu, J., Pickard, J. M. & Núñez, G. FDA-approved Disulfiram inhibits the NLRP3 inflammasome by regulating NLRP3 palmitoylation. *Cell. Rep.* **43** (8), 114609. https://doi.org/10.1016/j.celrep.2024.114609 (2024).
49. Qiu, K. & Kong, W. 1614-P: H2S improves skeletal muscle insulin resistance by inhibiting pyroptosis via Sirt2 pathway. *Diabetes* **73** (Supplement_1), 1614–P. https://doi.org/10.2337/db24-1614-P (2024).
50. Balakrishnan, R. & Thurmond, D. C. Mechanisms by which skeletal muscle myokines ameliorate insulin resistance. *Int. J. Mol. Sci.* **23** (9), 4636. https://doi.org/10.3390/ijms23094636 (2022).
51. Horii, T., Otsuka, M. & Yasu, T. Risk of non-hypoglycemic agents for hypoglycemia-related hospitalization in patients with type 2 diabetes: a large-scale medical receipt database analysis. *BMJ Open. Diabetes Res. Care.* **11** (2), e003177. https://doi.org/10.1136/bmjdrc-2022-003177 (2023).

Acknowledgements
We thank Mr. Matías Ayala for providing isolated muscle fibers and his valuable technical assistance.

Author contributions
Cynthia Cadagan : Writing – review & editing, Writing – original draft, Visualization, Supervision, Methodology, Investigation, Conceptualization, Formal analysis, Data curation. Javier Russell-Guzmán: Writing – review & editing, Writing – original draft, Visualization, Supervision, Methodology, Investigation, Conceptualization, Formal analysis, Data curation. Luan Americo da Silva: Writing – review & editing, Investigation, Formal analysis. Paula Montaña: Writing – review & editing, Methodology, Investigation, Formal analysis. Genaro Barrientos: Writing – review & editing, Investigation, Methodology. Sonja Buvinic : Writing – review & editing, Funding acquisition, Investigation. Gladys Tapia : Writing – review & editing, Supervision, Investigation. Manuel Estrada : Writing – review & editing, Writing – original draft, Visualization, Supervision. Paola Llanos : Writing – review & editing, Writing – original draft, Visualization, Supervision, Project administration, Investigation, Resources, Funding acquisition.

Funding
This work was supported by FONDECYT 1231103 (Paola Llanos) and 1241661 (Sonja Buvinic).

Declarations

Competing interests
The authors declare no competing interests.

Ethics approval
All animal experiments were approved by the Animal Bioethics Committee of the Faculty of Dentistry, University of Chile (Protocol CBA 240423 FOUCH).

Additional information
Supplementary Information The online version contains supplementary material available at https://doi.org/10.1038/s41598-025-30058-6.

Correspondence and requests for materials should be addressed to M.E. or P.L.